Bioorganic & Medicinal Chemistry 21 (2013) 388–394

Contents lists available at SciVerse ScienceDirect

Bioorganic & Medicinal Chemistry

journal homepage: www.elsevier.com/locate/bmc

Design, synthesis and molecular docking of α,β-unsaturated cyclohexanone analogous of curcumin as potent EGFR inhibitors with antiproliferative activity

Yun-Yun Xu [a,†], Yi Cao [b,†], Hailkuo Ma [a], Huan-Qiu Li [a,*], Gui-Zhen Ao [a,*]

[a] College of Pharmaceutical Science, Soochow University, Suzhou 215123, PR China
[b] School of Public Health, Soochow University, Suzhou 215123, PR China

ARTICLE INFO

Article history:
Received 9 October 2012
Revised 21 November 2012
Accepted 22 November 2012
Available online 2 December 2012

Keywords:
α,β-Unsaturated cyclohexanone analogous
Curcumin
EGFR
Antiproliferative
Molecular docking

ABSTRACT

A type of novel α,β-unsaturated cyclohexanone analogous, which designed based on the curcumin core structure, have been discovered as potential EGFR inhibitors. These compounds exhibit potent antiproliferative activity in two human tumor cell lines (Hep G2 and B16-F10). Among them, compounds **I_3** and **I_{12}** displayed the most potent EGFR inhibitory activity (IC_{50} = 0.43 μM and 1.54 μM, respectively). Molecular docking of **I_{12}** into EGFR TK active site was also performed. This inhibitor nicely fitting the active site might well explain its excellent inhibitory activity.

1. Introduction

Protein kinase plays a fundamental role in the aberrant signaling that is a hallmark of the uncontrolled proliferation of a variety of human tumors. So far they are considered as the second largest class of therapeutic targets. Among the growth factor receptor kinases that have been identified as being important in cancer is epidermal growth factor receptor (EGFR) kinase. Activation of EGFR may be because of overexpression, mutations resulting in constitutive activation, or autocrine expression of ligand.[1,2] Expression of a dominant negative Ras mutant in EGFR overexpressing cells also results in a significant potentiation of EGFR induced apoptosis suggesting that Ras activation is a key survival signal generated by the EGFR. The role of EGFR has been most thoroughly studied in breast cancer,[3] lung cancer (especially lung adenocarcinomas)[4–6] and in hormone-refractory prostate cancer.[7] Therefore, the EGFR kinase represents an attractive target for the development of novel therapies for the treatment of cancers. Several classes of inhibitors have been reported with the most potent and selective being the 4-(phenylamino)quinazolines.[8–10] Kinetic studies[11] show that these compounds selectively inhibit EGF-stimulated signal transduction by reversibly binding at the ATP site of EGFR. As we all know, three 4-(phenylamino)quinazolines, Gefitinb[12] (CP 358774), Erlotinib (ZD 1839)[13] and Lapatinib (GW572016)[14] are reported to be in clinical trial.

In the search for effective EGFR inhibitors, several natural product lead compounds had been identified. Curcumin (diferuloylmethane), the primary bioactive compound isolated from the rhizome of turmeric (Curcuma longa Linn.), is of particular interest.[15] Several clinical trials of curcumin are currently conducted in patients with pancreatic cancer, multiple myeloma, rheumatoid arthritis, cystic fibrosis, inflammatory bowel disease, psoriasis, and other disorders.[16,17] Curcumin has also been shown to downregulate the activity of EGFR and HER2 and to deplete cells of EGFR protein.[18–20] EGFR is expressed at high levels in colorectal cancer and prostate cancer. Curcumin inhibits the growth of human colon cancer-derived Moser cells by suppressing expression of the *cyclinD1* and EGFR genes.[21] Curcumin also downregulates EGFR signaling in prostate cancer cells by suppressing levels of EGFR protein, inhibiting the intrinsic EGFR tyrosine kinase activity, and attenuating ligand-induced activation of EGFR.[22]

Although curcumin is remarkably non-toxic and has promising anti-cancer activities, preclinical and clinical studies indicated that its poor bioavailability and pharmacokinetic profiles due to its instability under physiological conditions had limited its application in anti-cancer therapies.[23–25] For example, in a phase I trial, the concentrations of curcumin in plasma and target tissues were as low as 11.1 nM and 1.3 μM, respectively, even with an oral administration of 3.6 g/day.[17] Thus, our study focused on the improvement of its both pharmacokinetic profiles and bioavailability. It is suggested that the stability and metabolic profiles of curcumin could be enhanced by deleting the β-diketone moiety.

* Corresponding authors. Tel./fax: +86 512 65882092.
E-mail addresses: huanqiuli@suda.edu.cn (H.-Q. Li), aoguizhen@suda.edu.cn (G.-Z. Ao).
† Equally contributed to the work.

0968-0896/$ - see front matter © 2012 Elsevier Ltd. All rights reserved.
http://dx.doi.org/10.1016/j.bmc.2012.11.031

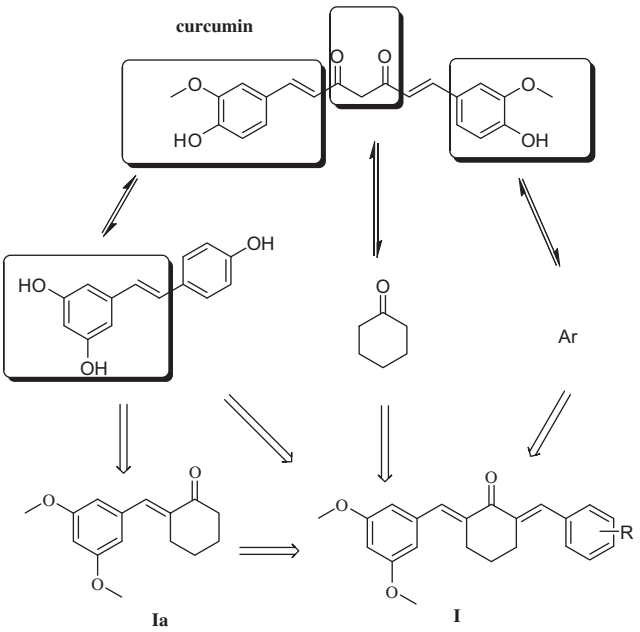

Figure 1. Design of the novel α,β-unsaturated cyclohexanone analogous.

Altering the β-diketone of curcumin with bioactive α, β-unsaturated cyclohexanone may increase the stability and antiproliferative activity. [25] Resveratrol, a phytoalexin is present in medicinal plants, grape skin, peanuts, and red wine, has the same stilbene structure and bioactivities with curcumin. Thus, a series of curcumin analogues had been designed through altering its β-diketones and aromatic ring, their structures contain both α, β-unsaturated cyclic ketone and phenolic hydroxyl of resveratrol (Fig. 1). Herein, we report the synthesis of α,β-unsaturated cyclohexanone analogous of curcumin, these compounds are potent in inhibition of cell growth in two cancer cell lines (Hep G2 and B16-F10) and with high levels of EGFR proteins and effectively induces apoptosis in a dose-dependent manner in the Hep G2 cell line, molecular docking was built to discuss the structure–activity relationship.

2. Results and discussion

2.1. Chemsitry

Twenty α,β-unsaturated cyclohexanone analogous of curcumin were designed and synthesized to be screened for the antiproliferative activity. All of them were synthesized for the first time. As show in Scheme 1, the intermediates **Ia** was prepared by the Stork reaction. Enamine **Ia**′ was synthesized by cyclohexanone and morpholine in benzene.

Ia was subsequently obtained by hydrolysis of 3,5-dimethoxybenzaldehyde and **Ia**′.

Then the α,β-unsaturated cyclohexanone analogous were synthesized by Claisen-Schimidt reaction, various substitute benzaldehydes and **Ia** were dissolved in 10% NaOH ethanol solution at room temperature to give the target compounds **I_1–I_{20}**. All compounds were purified by silicagel column and identified by elemental H and C NMR and HRMS.

The hydrolytic stabilities of the curcumin analogues were investigated in buffered 0.3% CMCNa solution at pH 7.4 and 37 °C in sodium dihydrogen phosphate buffer. The α,β-unsaturated cyclohexanone analogous lacking the β-diketone moiety were much more stable in the pH 7.4 situation. As a result, the stability of curcumin could be enhanced through deleting the β-diketone moiety.

Table 1
Structure of α, β-unsaturated cyclohexanone analogous and the biological effects

Compd	R	Antiproliferative assay IC_{50} (μM)		EGFR inhibition IC_{50} (μM)
		Hep G2	A16-F10	
I_1	Ph	4.74	2.45	1.6 ± 0.3
I_2	3-ClPh	6.11	5.17	2.2 ± 0.5
I_3	2-ClPh	5.67	3.23	1.5 ± 0.2
I_4	2-FPh	7.53	5.64	2.1 ± 0.4
I_5	2-BrPh	32.20	12.42	8.0 ± 1.6
I_6	3-BrPh	16.67	10.78	6.8 ± 1.8
I_7	4-BrPh	29.16	12.27	7.1 ± 0.9
I_8	4-FPh	12.09	7.63	5.6 ± 1.8
I_9	4-ClPh	25.48	18.41	15.3 ± 3.1
I_{10}	*c*-C_6H_{11}	17.17	12.21	7.5 ± 1.1
I_{11}	3-CH_3OPh	17.24	9.72	6.1 ± 1.2
I_{12}	3,4-diHOPh	1.01	0.71	0.4 ± 0.1
I_{13}	2-CH_3OPh	>100	>100	20.8 ± 4.9
I_{14}	4-HOPh	10.47	3.28	4.6 ± 0.5
I_{15}	4-$(CH_3)_2$NPh	11.76	5.84	3.9 ± 0.2
I_{16}	3-HO-4-CH_3OPh	11.05	7.04	5.3 ± 0.7
I_{17}	4-CH_3OPh	58.07	32.65	18.6 ± 2.2
I_{18}	3,5-Di CH_3OPh	8.56	4.71	2.0 ± 0.4
I_{19}	4-CH_3SO_2Ph	6.68	3.58	1.9 ± 0.2
I_{20}	3,5-$(CH_3)_3$C-4-HOPh	11.11	7.69	4.8 ± 0.6
Curcumin		26.99	18.65	8.6 ± 2.1
Erlotinib		0.12	0.2	0.03

2.2. Antiproliferative activity in vitro

The synthesizedα, β-unsaturated cyclohexanone analogous of curcumin were evaluated for their antiproliferative activities against Hep G2 and B16-F10 cells by applying the MTT colorimetric assay. The results were summarized in Table 1. As expected, most α,β-unsaturated cyclohexanone analogous exhibited remarked effects on antiproliferative activities, and generally the results showed which those applied to B16-F10 cells would performed better than that in Hep G2 cells. Especially, (2*E*,6*E*)-2-(3,5-dihydroxybenzylidene)-6-(3,5-dimethoxybenzylidene)cyclohexanone (**I_{12}**) showed themost potent inhibitory activity (IC_{50} = 1.01 μM for Hep G2 and IC_{50} = 0.71 μM for B16-F10), much better than curcumin (IC_{50} = 26.99 μM for Hep G2 and IC_{50} = 18.65 μM for B16-F10) and comparable to the positive control erlotinib.

Preliminary SAR (Structure activity relationship) studies were performed to deduce how the structure variation and modification could affect the antiproliferative activity. Firstly, a main trend was

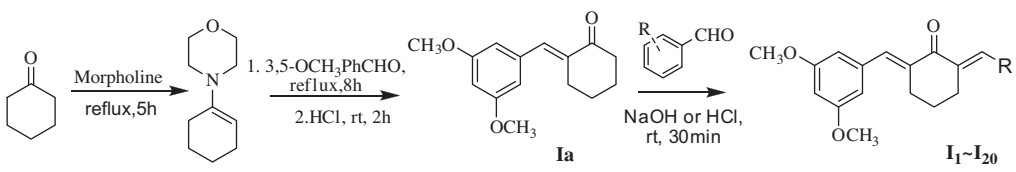

Scheme 1. Synthetic routes of α, β-unsaturated cyclohexanone analogous **I_1–I_{20}**.

that compounds with hydroxyl substitution on *R*-phenyl ring ($\mathbf{I_{12}}$ and $\mathbf{I_{14}}$) displayed more potent antiproliferative activity compared to other compounds, while compounds with methoxyl substitution on *R*-phenyl ring ($\mathbf{I_{11}}$ and $\mathbf{I_{13}}$) did not input substantial effects on the antiproliferative capability, so the increased lipophilicity of methoxy derivatives at R1 position may be detrimental to the inhibitory activity.

Secondly, as for compounds with halogen substitution on *R*-phenyl ring, we could perceive the tendency that Cl ⩾ F > Br in the series. Compounds with R1 substitution at the *meta* position ($\mathbf{I_2}$, $\mathbf{I_6}$, $\mathbf{I_{11}}$ and $\mathbf{I_{16}}$) showed better activities than those with substitution at the *para* position ($\mathbf{I_7}$, $\mathbf{I_8}$, $\mathbf{I_9}$ and $\mathbf{I_{14}}$) based both on cytotoxicity and enzyme inhibitory activity, respectively. Taken together, the designed and synthesized curcumin α,β-unsaturated cyclohexanone analogous did demonstrate fairly potent antiproliferative activity against two tested cancer cell lines. Therefore, more structurally diversified derivatives would be synthesized and evaluated to provide clues on the antagonist–protein interaction.

2.3. EGFR inhibitory activity and molecular docking

To evaluate the EGFR inhibitory potency of new compounds, their ability to block EGFR was tested in an EGFR TK assay, their EGFR inhibitory activities were displayed at Table 1. This result basically correlates well with that from the cancer cell based assay. As shown in Table 1, compounds $\mathbf{I_3}$ and $\mathbf{I_{12}}$ displayed the most potent inhibitory activity (IC_{50} = 0.43 μM and 1.54 μM for EGFR), less comparable to the positive control erlotinib (IC_{50} = 0.03 μM for EGFR). This biological assay indicated thatα, β-unsaturated cyclohexanone analogous $\mathbf{I_{12}}$ and $\mathbf{I_3}$ are potential small-molecule EGFR inhibitors as anticancer agents.

In order to explore probable interaction model of inhibitors and enzyme active site, molecular docking of the most potent inhibitor $\mathbf{I_{12}}$ into ATP binding site of EGFR kinase was performed on the binding model based on the EGFR complex structure (1M17.pdb). All docking runs were applied CDOCKER protocol of Discovery Studio 3.1. The 2D and 3D binding model of compound $\mathbf{I_{12}}$ and EGFR was depicted in Figure 2. In the binding model, compound $\mathbf{I_{12}}$ is nicely bound to the region of EGFR with binding interaction energy of −51.38 KJ mol^{-1}. Visual inspection of the pose of $\mathbf{I_{12}}$ into the active site revealed that an optimal intermolecular hydrogen bond were observed (ASP776: N–H···O: 2.3 Å, angle: 137.6°). The modeling also suggested that there is a π-cation interaction between benzene ring of compound $\mathbf{I_{12}}$ and the side chain of LYS721, π-cation interaction energies are of the same order of magnitude as hydrogen bonds or salt bridges and play an important role in stabilizing the three dimensional structure of a protein.[26]

2.4. Analysis of apoptosis induced by compounds I12

We evaluated compound $\mathbf{I_{12}}$ for their ability to induce apoptosis in the Hep G2 cell line using Annexin-V and propium iodide (PI) double staining by flow cytometry.

The results are shown in Figure 3. As can be seen, compound $\mathbf{I_{12}}$ is effective in induction of apoptosis in a dose-dependent manner. Treatment of the Hep G2 cells by 1 and 2 μM of $\mathbf{I_{12}}$ for 3 days results in 32.8% and 39.8% of apoptotic cells (early + late), as compared to 0.98% of apoptotic cells in an untreated control. This is consistent with its nice binding affinity to EGFR TK and its potent activity in inhibition of cell growth.

3. Conclusion

In this study, a series of α,β-unsaturated cyclohexanone analogous of curcumin were synthesized and evaluated for inhibitory activity against EGFR TK kinases as well as antiproliferative activity of two cancer cell lines. As expected, these compounds exhibited remarkable effects on antiproliferative activity and EGFR TK inhibitory activity. Especially, compound $\mathbf{I_{12}}$ showed the most potent inhibitory activity (IC_{50} = 1.01 μM for Hep G2 and IC_{50} = 0.71 μM for B16-F10), much better than that of curcumin (IC_{50} = 26.99 μM for Hep G2 and IC_{50} = 18.65 μM for B16-F10) and comparable to the positive control erlotinib. The EGFR molecular docking model suggested that compound $\mathbf{I_{12}}$ is nicely bound to the region of EGFR. Thus, compound $\mathbf{I_{12}}$ is potent EGFR TK inhibitor and effectively induces apoptosis in a dose-dependent manner in the Hep G2 cell line as a potential antiproliferative agent.

4. Experimental section

4.1. General chemistry

All chemicals (reagent grade) used were purchased from Sigma–Aldrich (USA) and Sinopharm Chemical Reagent Co., Ltd.

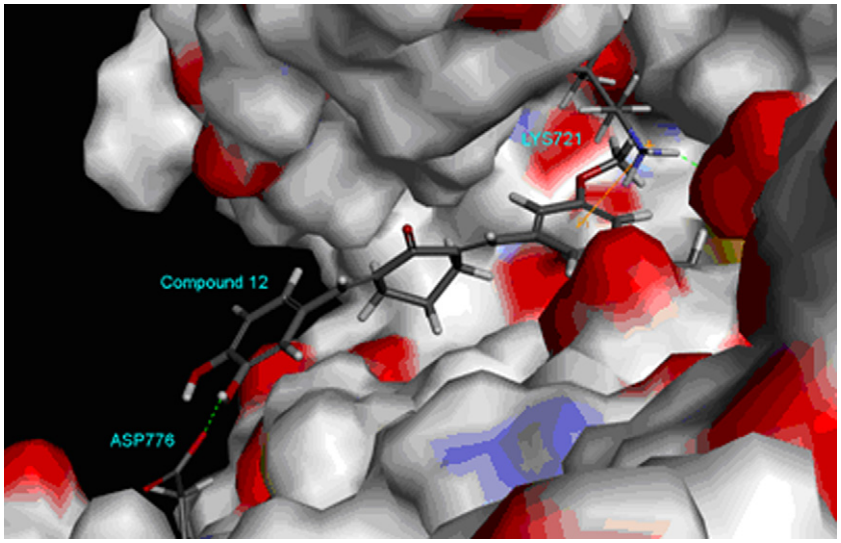

Figure 2. The 3D model structure of compound $\mathbf{I_{12}}$ binding model with EGFR TK complex. (PDB ID: 1M17) using Discovery Studio program with the essential amino acid residues at the binding site are tagged in circles. The purple circles show the amino acids which participate in hydrogen bonding, electrostatic or polar interactions and the green circles show the amino acids which participate in the Van der Waals interactions.

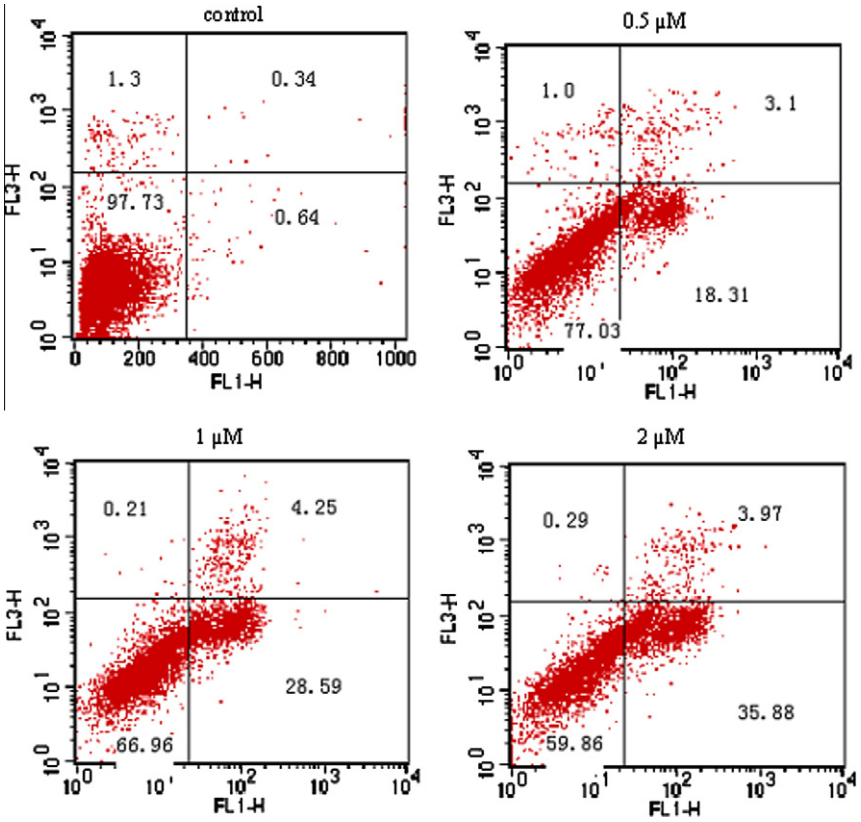

Figure 3. Analysis of apoptosis induced by compounds $\mathbf{I_{12}}$ in the Hep G2 liver cancer cell line. Data represent the percentage of apoptotic cells. (a) control, (b) 0. 5 μM, (c) 1.0 μM, (d) 2.0 μM.

(China). ^{1}H NMR spectra were measured on Varian Unity Inova 300/400 MHz NMR Spectrometer at 25 °C and referenced to TMS. Chemical shifts are reported in ppm (d) using the residual solvent line as internal standard. Splitting patterns are designed as s, singlet; d, doublet; t, triplet; m, multiplet. HRMS spectra were acquired on Bruker Esquire Liquid Chromatography-Ion Trap Mass Spectrometer. Analytical thin-layer chromatography (TLC) was performed on the glass-backed silica gel sheets (silica gel 60 Å GF254). All compounds were detected using UV light (254 or 365 nm). Analytical HPLC was conducted on SHIMADZU LC-20AD. Prior to biological evaluation, all compounds were determined to be >95% pure using appropriate analytical methods (MeOH/H_2O 80% v/v, MeOH/H_2O 75% v/v, MeOH/H_2O 60% v/v) based on the peak area percentage.

4.2. General procedure for the preparation of compounds

Various substitute benzaldehydes (1.22 mmol) and **Ia** (300 mg, 1.22 mmol) were dissolved in 10% NaOH ethanol solution (10 ml), and stirring at rt for 30 min. Then water (50 ml) was added, the product extraction was carried out with EtOAc (3 × 20 ml). The organic layer was dried over Na_2SO_4, and after solvent evaporation the residue was purified by flash column chromatography (silica gel 60, 35–70 mesh) using $CHCl_3$ as the eluent.

4.2.1. (2*E*,6*E*)-2-Benzylidene-6-(3,5-dimethoxybenzylidene)-cyclohexanone ($\mathbf{I_1}$)

Mp: 90.2–91.0 °C. Yield: 87%; ^{1}H NMR (400 MHz, $CDCl_3$), δ (ppm): 7.80 (s, 1H, =CH), 7.72 (s, 1H, =CH), 7.47 (m, 2H, ArH), 7.41 (t, 2H, J = 7.2 Hz, ArH), 7.35 (t, 1H, J = 7.1 Hz, ArH), 6.60 (d, 2H, J = 1.8 Hz, ArH), 6.46 (s, 1H, ArH), 3.82 (s, 6H, OCH_3), 2.92 (t, 4H, J = 5.7 Hz, CH_2), 1.79 (quint, 2H, J = 6.1 Hz, CH_2). ^{13}C NMR (400 MHz, $CDCl_3$), δ (ppm): 190.529, 160.834, 138.020, 137.278, 137.123, 136.898, 136.406, 136.196, 130.653, 128.891, 128.657, 108.582, 101.032, 55.673, 28.802, 28.721, 23.229. HR-MS: Calcd For $C_{21}H_{20}O_3[M+H]^+$: 321.1485. Found: 321.1475.

4.2.2. (2*E*,6*E*)-2-(3-Chlorobenzylidene)-6-(3,5-dimethoxybenzylidene)cyclohexanone ($\mathbf{I_2}$)

Mp: 107.5–108.4 °C. Yield: 84%; ^{1}H NMR (400 MHz, $CDCl_3$), δ (ppm): 7.72 (s, 1H, =CH), 7.70 (s, 1H, =CH), 7.43 (s, 1H, ArH), 7.33 (m, 3H, ArH), 6.61 (d, 2H, J = 2.1 Hz, ArH), 6.47 (t, 1H, J = 2.1 Hz, ArH), 3.82 (s, 6H, OCH_3), 2.92 (m, 4H, CH_2), 1.81 (quint, 2H, J = 6.5 Hz, CH_2). ^{13}C NMR(400 MHz, $CDCl_3$), δ (ppm): 190.257, 160.841, 137.985, 137.876, 137.577, 137.541, 136.631, 135.558, 134.564, 130.172, 129.936, 128.795, 108.625, 101.106, 55.707, 28.762, 28.684, 23.117. HR-MS: Calcd For $C_{22}H_{21}ClO_3$ $[M+H]^+$: 369.1252, Found: 369.1257.

4.2.3. (2*E*,6*E*)-2-(2-Chlorobenzylidene)-6-(3,5-dimethoxybenzylidene)cyclohexanone ($\mathbf{I_3}$)

Mp: 104.0–104.7 °C. Yield: 82%; ^{1}H NMR (400 MHz, $CDCl_3$), δ (ppm): 7.88 (s, 1H, =CH), 7.74 (s, 1H, =CH), 7.44 (m, 1H, ArH), 7.33 (m, 1H, ArH), 7.28 (m, 2H, ArH), 6.61 (d, 2H, J = 2.0 Hz, ArH), 6.47 (t, 1H, J = 2.1 Hz, ArH), 3.82 (s, 6H, OCH_3), 2.94 (t, 2H, J = 5.6 Hz, CH_2), 2.76 (t, 2H, J = 5.5 Hz, CH_2), 1.77 (quint, 2H, J = 6.2 Hz, CH_2). ^{13}C NMR (400 MHz, $CDCl_3$), δ (ppm): 190.280, 160.837, 138.169, 137.948, 137.752, 136.739, 135.260, 134.694, 133.913, 130.818, 130.009, 129.827, 126.555, 108.627, 101.090, 55.706, 28.983, 28.483, 23.363.HR-MS: Calcd For $C_{22}H_{21}ClO_3$ $[M+H]^+$: 369.1252, Found: 369.1251.

4.2.4. (2*E*,6*E*)-2-(3,5-Dimethoxybenzylidene)-6-(2-fluorobenzylidene)cyclohexanone ($\mathbf{I_4}$)

Mp: 83.0–83.6 °C. Yield: 85%; ^{1}H NMR (400 MHz, $CDCl_3$), δ (ppm): 7.82 (s, 1H, =CH), 7.72 (s, 1H, =CH), 7.30–7.39 (m, 2H,

ArH), 7.16 (t, 1H, J = 7.5 Hz, ArH), 7.11 (t, 1H, J = 9.3 Hz, ArH), 6.60 (d, 2H, J = 2.1 Hz, ArH), 6.47 (t, 1H, J = 2.0 Hz, ArH), 3.82 (s, 6H, OCH_3), 2.94 (t, 2H, J = 5.4 Hz, CH_2), 2.80 (t, 2H, J = 5.8 Hz, CH_2), 1.78 (quint, 2H, J = 6.5 Hz, CH_2). ^{13}C NMR (400 MHz, $CDCl_3$), δ (ppm): 190.173, 160.836, 138.570, 137.967, 137.597, 136.772, 131.009, 130.670, 130.589, 129.727, 124.009, 116.154, 115.937, 108.617, 101.088, 55.715, 28.953, 28.749, 23.246. HR-MS: Calcd. For $C_{22}H_{21}FO_3$ $[M+H]^+$: 353.1547, Found: 353.1549.

4.2.5. (2*E*,6*E*)-2-(2-Bromobenzylidene)-6-(3,5-dimethoxybenzylidene)cyclohexanone (I_5)

Mp: 111.7–112.5 °C. Yield: 81%; ^1H NMR (400 MHz, $CDCl_3$), δ (ppm): 7.82 (s, 1H, =CH), 7.74(s, 1H, =CH), 7.63 (d, 1H, J = 7.9 Hz, ArH), 7.30 (m, 2H, ArH), 7.20 (t, 1H, J = 8.0 Hz, ArH), 6.60 (d, 2H, J = 1.9 Hz, ArH), 6.47 (t, 1H, J = 1.9 Hz, ArH), 3.82(s, 6H, $-OCH_3$), 2.93 (t, 2H, J = 5.6 Hz, $-CH_2$), 2.74 (t, 2H, J = 5.3 Hz, $-CH_2$), 1.77 (quint, 2H, J = 6.5 Hz, $-CH_2$). ^{13}C NMR (400 MHz, $CDCl_3$), δ (ppm): 190.273, 160.844, 137.958, 137.894, 137.796, 136.730, 136.559, 136.196, 133.208, 130.848, 129.961, 127.178, 125.408, 108.638, 101.102, 55.720, 28.996, 28.381, 23.362. HR-MS: Calcd. For $C_{22}H_{21}BrO_3$ $[M+H]^+$: 413.0747, Found: 413.0765.

4.2.6. (2*E*,6*E*)-2-(3-Bromobenzylidene)-6-(3,5-dimethoxybenzylidene)cyclohexanone (I_6)

Mp: 111.9–112.7 °C. Yield: 87%; ^1H NMR (400 MHz, $CDCl_3$), δ (ppm): 7.72 (s, 1H, =CH), 7.69 (s, 1H, =CH), 7.59 (s, 1H, ArH), 7.46 (d, 1H, J = 7.7 Hz, ArH), 7.36 (d, 1H, J = 7.6 Hz, ArH), 7.28 (t, 1H, J = 7.9 Hz, ArH), 6.60 (s, 2H, ArH), 6.47 (s, 1H, ArH), 3.82 (s, 6H, OCH_3), 2.91 (m, 4H, CH_2), 1.79 (quint, 2H, J = 6.3 Hz, CH_2). ^{13}C NMR (400 MHz, $CDCl_3$), δ (ppm): 190.151, 160.825, 138.269, 137.846, 137.558, 136.593, 135.402, 133.047, 131.667, 130.167, 129.157, 122.721, 108.617, 101.105, 55.676, 28.728, 28.622, 23.097. HR-MS: Calcd. For $C_{22}H_{21}BrO_3$ $[M+H]^+$: 413.0747, Found: 413.0747.

4.2.7. (2*E*,6*E*)-2-(4-Bromobenzylidene)-6-(3,5-dimethoxybenzylidene)cyclohexanone (I_7)

Mp: 126.4–128.6 °C. Yield: 83%; ^1H NMR (400 MHz, $CDCl_3$), δ (ppm): 7.71 (s, 1H, =CH), 7.70 (s, 1H, =CH), 7.53 (d, 2H, J = 8.3 Hz, ArH), 7.32 (d, 2H, J = 8.3 Hz, ArH), 6.60 (d, 2H, J = 1.8 Hz, ArH), 6.47 (s, 1H, ArH), 3.82 (s, 6H, OCH_3), 2.93 (t, 2H, J = 5.4 Hz, CH_2), 2.88 (t, 2H, J = 5.4 Hz, CH_2), 1.79 (quint, 2H, J = 6.4 Hz, CH_2). ^{13}C NMR (400 MHz, $CDCl_3$), δ (ppm): 190.323, 160.845, 137.912, 137.454, 136.967, 136.685, 135.922, 135.069, 132.115, 131.905, 123.159, 108.617, 101.084, 55.718, 28.755, 23.137. HR-MS: Calcd For $C_{22}H_{21}BrO_3$ $[M+H]^+$: 413.0747, Found: 413.0761.

4.2.8. (2*E*,6*E*)-2-(3,5-Dimethoxybenzylidene)-6-(4-fluorobenzylidene)cyclohexanone (I_8)

Mp: 107.2–108.3 °C. Yield: 77%; ^1H NMR (400 MHz, $CDCl_3$), δ (ppm): 7.73 (s, 1H, =CH), 7.70 (s, 1H, =CH), 7.44 (d, 2H, J = 8.6 Hz, ArH), 7.08 (d, 2H, J = 8.5 Hz, ArH), 6.59 (d, 2H, J = 1.7 Hz, ArH), 6.45 (s, 1H, ArH), 3.80 (s, 6H, OCH_3), 2.86–2.93 (m, 4H, CH_2), 1.78 (quint, 2H, J = 6.1 Hz, CH_2). ^{13}C NMR (400 MHz, $CDCl_3$), δ (ppm): 190.421, 160.876, 137.996, 137.260, 136.801, 136.156, 132.622, 132.540, 132.375, 115.923, 115.709, 108.616, 101.072, 55.708, 28.765, 28.702, 23.196. HR-MS: Calcd For $C_{22}H_{21}FO_3$ $[M+H]^+$: 353.1547, Found: 353.1575.

4.2.9. (2*E*,6*E*)-2-(4-Chlorobenzylidene)-6-(3,5-dimethoxybenzylidene)cyclohexanone (I_9)

Mp: 124.4–124.8 °C. Yield: 84%; ^1H NMR (400 MHz, $CDCl_3$), δ (ppm): 7.72 (s, 1H, =CH), 7.71 (s, 1H, =CH), 7.38 (m, 4H, ArH), 6.60 (d, 2H, J = 2.1 Hz, ArH), 6.47 (t, 1H, J = 2.1 Hz, ArH), 3.82 (s, 6H, OCH_3), 2.93 (t, 2H, J = 5.6 Hz, CH_2), 2.87 (t, 2H, J = 5.5 Hz, CH_2), 1.79 (quint, 2H, J = 6.5 Hz, CH_2). ^{13}C NMR (400 MHz, $CDCl_3$), δ (ppm): 190.341, 160.852, 137.923, 137.417, 136.847, 136.702, 135.900, 134.816, 134.636, 131.895, 128.949, 108.613, 101.074, 55.713, 28.752, 23.144. HR-MS: Calcd For $C_{22}H_{21}ClO_3$ $[M+H]^+$: 369.1252, Found: 369.1269.

4.2.10. (2*E*,6*E*)-2-(Cyclohexylmethylene)-6-(3,5-dimethoxybenzylidene)cyclohexanone (I10)

Mp: 94.0–95.1 °C. Yield: 86%; ^1H NMR (400 MHz, $CDCl_3$), δ (ppm): 7.64 (s, 1H, =CH), 6.73 (d, 1H, J = 9.8 Hz, ArH), 6.60 (d, 2H, J = 1.9 Hz, ArH), 6.45 (s, 1H, ArH), 3.81 (s, 6H, OCH_3), 2.86 (t, 2H, J = 5.6 Hz, CH_2), 2.60 (t, 2H, J = 5.5 Hz, CH_2), 2.29 (m, 1H, CH), 1.74–1.77 (m, 4H, CH_2), 1.67 (m, 2H, CH_2), 1.14–1.35 (m, 6H, CH_2). ^{13}C NMR (400 MHz, $CDCl_3$), δ (ppm): 190.633, 160.785, 146.497, 138.165, 137.117, 136.557, 134.262, 108.505, 100.872, 55.694, 37.558, 32.046, 28.853, 26.466, 26.180, 25.941, 23.040. HR-MS: Calcd For $C_{22}H_{28}O_3$ $[M+H]^+$: 341.2111, Found: 341.2111.

4.2.11. (2*E*,6*E*)-2-(3,5-Dimethoxybenzylidene)-6-(3-methoxybenzylidene)cyclohexanone (I_{11})

Mp: 92.0–92.6 °C. Yield: 83%; ^1H NMR δ (ppm): 7.76 (s, 1H, =CH), 7.71 (s, 1H, =CH), 7.32 (t, 1H, J = 7.9 Hz, ArH), 7.06 (d, 1H, J = 7.7 Hz, ArH), 7.00 (s, 1H, ArH), 6.90 (d, 1H, J = 8.2 Hz, ArH), 6.60 (d, 2H, J = 1.6 Hz, ArH), 6.50 (s, 1H, ArH), 3.84 (s, 3H, CH_3), 3.82 (s, 6H, OCH_3), 2.90 (t, 4H, J = 5.2 Hz, CH_2), 1.80 (quint, 2H, J = 6.4 Hz, CH_2). ^{13}C NMR δ (ppm): 190.429, 160.792, 159.652, 137.955, 137.471, 137.107, 136.832, 136.619, 129.600, 123.085, 116.005, 114.455, 108.548, 100.994, 55.630, 55.507, 28.755, 28.728, 23.156. HR-MS: Calcd For $C_{23}H_{24}O_4$ $[M+H]^+$: 365.1747, Found: 365.1747.

4.2.12. (2*E*,6*E*)-2-(3,4-Dihydroxybenzylidene)-6-(3,5-dimethoxybenzylidene)cyclohexanone (I_{12})

Mp: 157.6–158.7 °C. Yield: 91%; ^1H NMR δ (ppm): 7.79 (s, 1H, =CH), 7.71 (s, 1H, =CH), 7.19 (s, 1H, ArH), 7.04 (d, 1H, J = 8.3 Hz, ArH), 6.93 (d, 1H, J = 8.2 Hz, ArH), 6.60 (s, 2H, ArH), 6.47 (d, 1H, J = 1.6 Hz, ArH), 3.82 (d, 6H, J = 1.6 Hz, OCH_3), 2.90 (m, 4H, CH_2), 1.79 (quint, 2H, J = 5.7 Hz, CH_2). ^{13}C NMR δ (ppm): 189.808, 160.872, 147.521, 145.617, 137.848, 137.753, 137.630, 135.768, 133.608, 127.474, 124.263, 118.335, 116.360, 108.601, 101.240, 55.840, 28.557, 28.367, 22.934. HR-MS: Calcd For $C_{22}H_{22}O_5$ $[M+H]^+$: 367.1540, Found: 367.1541.

4.2.13. (2*E*,6*E*)-2-(3,5-Dimethoxybenzylidene)-6-(2-methoxybenzylidene)cyclohexanone (I_{13})

Mp: 90.8–91.2 °C. Yield: 85%; ^1H NMR δ (ppm): 7.99 (s, 1H, =CH), 7.71 (s, 1H, =CH), 7.33 (m, 2H, ArH), 6.97 (t, 1H, J = 7.4 Hz, ArH), 6.92 (d, 1H, J = 8.2 Hz, ArH), 6.60 (d, 2H, J = 2.0 Hz, ArH), 6.46 (t, 1H, J = 2.0 Hz, ArH), 3.87 (s, 3H, OCH_3), 3.82 (s, 6H, OCH_3), 2.92 (t, 2H, J = 5.7 Hz, CH_2), 2.84 (t, 2H, J = 5.5 Hz, CH_2), 1.77 (quint, 2H, J = 6.2 Hz, CH_2). ^{13}C NMR δ (ppm): 190.502, 160.769, 158.596, 138.117, 137.105, 136.911, 136.417, 132.909, 130.533, 130.388, 125.110, 120.152, 110.817, 108.510, 100.880, 55.686, 55.611, 28.956, 28.735, 23.421. HR-MS: Calcd For $C_{23}H_{24}O_4$ $[M+H]^+$: 365.1747, Found: 365.1750.

4.2.14. (2*E*,6*E*)-2-(3,5-Dimethoxybenzylidene)-6-(4-hydroxybenzylidene)cyclohexanone (I_{14})

Mp: 155.0–155.6 °C. Yield: 84%; ^1H NMR δ (ppm): 7.76 (s, 1H, =CH), 7.72 (s, 1H, =CH), 7.39 (d, 2H, J = 8.3 Hz, ArH), 6.90 (d, 2H, J = 8.4 Hz, ArH), 6.59 (s, 2H, ArH), 6.46 (s, 1H, ArH), 6.27 (s, 1H, OH), 3.81 (s, 6H, OCH_3), 2.90 (m, 4H, CH_2), 1.79 (m, 2H, CH_2). ^{13}C NMR δ (ppm): 191.373, 160.838, 157.381, 138.314, 138.045, 137.259, 137.102, 134.065, 133.039, 128.507, 115.982, 108.648,

101.149, 55.748, 28.860, 28.718, 23.219. HR-MS: Calcd For $C_{22}H_{22}O_4$ $[M+H]^+$: 351.1591, Found: 351.1590.

4.2.15. (2*E*,6*E*)-2-(3,5-Dimethoxybenzylidene)-6-(4-(dimethylamino)benzylidene)cyclohexanone (I_{15})

Mp: 109.6–110.3 °C. Yield: 80%; ^{1}H NMR δ (ppm): 7.78 (s, 1H, =CH), 7.70 (s, 1H, =CH), 7.46 (d, 2H, J = 8.8 Hz, ArH), 6.72 (d, 2H, J = 8.8 Hz, ArH), 6.60 (d, 2H, J = 2.0 Hz, ArH), 6.44 (s, 1H, ArH), 3.81 (s, 6H, OCH_3), 3.03 (s, 6H, NCH_3), 2.95 (t, 2H, J = 6.3 Hz, CH_2), 2.90 (t, 2H, J = 5.6 Hz), 1.80 (quint, 2H, J = 6.2 Hz, CH_2). ^{13}C NMR δ (ppm): 190.267, 160.794, 150.851, 138.751, 138.411, 137.439, 135.885, 133.004, 131.900, 124.155, 111.895, 108.468, 100.776, 55.675, 40.389, 29.099, 28.733, 23.333. HR-MS: Calcd For $C_{24}H_{27}NO_3$ $[M+H]^+$: 378.2064, Found: 378.2060.

4.2.16. (2E,6E)-2-(3,5-Dimethoxybenzylidene)-6-(3-hydroxy-4-methoxybenzylidene)cyclohexanone (I_{16})

Mp: 131.2–131.6 °C. Yield: 79%; ^{1}H NMR δ (ppm): 7.72 (s, 1H, =CH), 7.69 (s, 1H, =CH), 7.01 (d, 1H, J = 8.2 Hz, ArH), 6.97 (s, 1H, ArH), 6.93 (d, 1H, J = 8.2 Hz, ArH), 6.58 (d, 2H, J = 1.5 Hz, ArH), 6.43 (s, 1H, ArH), 5.86 (s, 1H, OH), 3.90 (s, 3H, OCH_3), 3.79 (s, 6H, OCH_3), 2.87 (m, 4H, CH_2), 1.77 (quint, 2H, J = 6.2 Hz, CH_2). ^{13}C NMR δ (ppm): 190.406, 160.764, 146.897, 146.642, 138.046, 137.833, 136.960, 136.735, 134.218, 128.600, 124.835, 114.805, 113.616, 108.524, 100.915, 56.175, 55.635, 28.827, 28.664, 23.182. HR-MS: Calcd For $C_{23}H_{24}O_5$ $[M+H]^+$: 381.1697, Found: 381.1692.

4.12.17. (2*E*,6*E*)-2-(3,5-Dimethoxybenzylidene)-6-(4-methoxybenzylidene)cyclohexanone (I_{17})

Mp: 97.7–98.1 °C. Yield: 82%; ^{1}H NMR δ (ppm): 7.77(s, 1H, =CH), 7.71 (s, 1H, =CH), 7.46 (d, 2H, J = 8.7 Hz, ArH), 6.94 (d, 2H, J = 8.7 Hz, ArH), 6.60(d, 2H, J = 1.9 Hz, ArH), 6.46 (s, 1H, ArH), 3.85 (s, 3H, CH_3), 3.82 (s, 6H, OCH_3), 2.92 (t, 4H, J = 5.9 Hz, CH_2), 1.80 (quint, 2H, J = 6.4 Hz, CH_2). ^{13}C NMR δ (ppm): 190.280, 160.745, 160.225, 138.045, 137.273, 136.970, 136.560, 134.257, 132.562, 128.771, 114.127, 108.460, 100.849, 55.573, 28.774, 28.657, 23.150. HR-MS: Calcd. For $C_{23}H_{24}O_4$ $[M+H]^+$: 365.1747, Found: 365.1747.

4.2.18. (2*E*,6*E*)-2,6-Bis(3,5-dimethoxybenzylidene)-cyclohexanone (I_{18})

Mp: 135.7–136.5 °C. Yield: 78%; ^{1}H NMR δ (ppm): 7.71 (s, 2H, =CH), 6.60 (d, 4H, J = 2.1 Hz, ArH), 6.46 (t, 2H, J = 2.1 Hz, ArH), 3.82 (s, 12H, OCH_3), 2.92 (t, 4H, J = 5.5 Hz, CH_2), 1.78 (quint, 2H, J = 6.6 Hz, CH_2). ^{13}C NMR δ (ppm): 190.525, 160.833, 137.995, 137.243, 136.866, 108.592, 101.041, 55.702, 28.813, 23.181. HR-MS: Calcd For $C_{24}H_{26}O_5$ $[M+H]^+$: 395.1853, Found: 395.1869.

4.2.19. (2*E*,6*E*)-2-(3,5-Dimethoxybenzylidene)-6-(4-(methylsulfonyl)benzylidene)cyclohexanone (I_{19})

Mp: 162.0–163.5 °C. Yield: 86%; ^{1}H NMR δ (ppm): 7.79 (d, 2H, J = 8.2 Hz, ArH), 7.76 (s, 1H, =CH), 7.73 (s, 1H, =CH), 7.61 (d, 2H, J = 8.2 Hz, ArH), 6.61 (s, 2H, ArH), 6.48 (s, 1H, ArH), 3.82 (s, 6H, OCH_3), 3.09 (s, 3H, SO_2CH_3), 2.95 (t, 2H, J = 5.1 Hz, CH_2), 2.89 (t, 2H, J = 5.3 Hz, CH_2), 1.80 (quint, 2H, J = 5.6 Hz,CH_2). ^{13}C NMR δ (ppm): 189.744, 160.713, 141.522, 139.929, 139.108, 137.843, 137.523, 136.255, 134.311, 130.899, 127.501, 108.540, 101.071, 55.543, 44.536, 28.541, 28.499, 22.860. HR-MS: Calcd For $C_{23}H_{24}O_5S$ $[M+H]^+$: 413.1417, Found: 413.1396.

4.2.20. (2*E*,6*E*)-2-(3,5-Di-*tert*-butyl-4-hydroxybenzylidene)-6-(3,5-dimethoxybenzylidene)cyclohexanone (I_{20})

Mp: 148.2–149.9 °C. Yield: 82%; ^{1}H NMR δ (ppm): 7.79 (s, 1H, =CH), 7.70 (s, 1H, =CH), 7.37 (s, 2H, ArH), 6.60 (s, 2H, ArH), 6.45 (s, 1H, ArH), 5.48 (s, 1H, OH), 3.82 (s, 6H, OCH_3), 2.903 (m, 4H, CH_2), 1.80 (quint, 2H, J = 5.8 Hz, CH_2), 1.46 (s, 18H, CH_3). ^{13}C NMR δ (ppm): 190.493, 160.829, 155.078, 139.015, 138.272, 137.232, 136.481, 136.151, 133.471, 128.514, 127.638, 108.539, 100.878, 55.704, 34.704, 30.539, 28.925, 28.785, 23.435. HR-MS: Calcd For $C_{30}H_{38}O_4$ $[M+H]^+$: 463.2843, Found: 463.2829.

4.3. Cell proliferation assay

The antiproliferative activities of chalcone thiosemicarbazide derivatives were determined using a standard (MTT)-based colorimetric assay (Sigma). Briefly, cell lines were seeded at a density of 7×103 cells/well in 96-well microtiter plates (Costar). After 24 h, exponentially growing cells were exposed to the indicated compounds at final concentrations ranging from 0.1 to 40 mg/mL. After 48 h, cell survival was determined by the addition of an MTT solution (20 μL of 5 mg/mL MTT in PBS). After 6 h, 100 mL of 10% SDS in 0.01 N HCl was added, and the plates were incubated at 37 °C for a further 4 h; optical absorbance was measured at 570 nm on an LX300 Epson Diagnostic microplate reader. Survival ratios are expressed in percentages with respect to untreated cells. IC_{50} values were determined from replicates of 6 wells from at least two independent experiments.

4.4. General procedure for preparation, purification of EGFR inhibitory assay

1.6 kb cDNA encoded for the EGFR cytoplasmic domain (EGFR-CD, amino acids 645–1186) were cloned into baculoviral expression vectors pBlueBacHis2B and pFASTBacHTc, separately. A sequence that encodes $(His)_6$ was located at the 5′ upstream to the EGFR sequence. Sf-9 cells were infected for 3 days for protein expression. Sf-9 cell pellets were solubilized at 0 °C in a buffer at pH 7.4 containing 50 mM HEPES, 10 mM NaCl, 1% Triton, 10 μM ammonium molybdate, 100 μM sodium vanadate, 10 μg/mL aprotinin, 10 μg/mL leupeptin, 10 μg/mL pepstatin, and 16 μg/mL benzamidine HCl for 20 min followed by 20 min centrifugation. Crude extract supernatant was passed through an equilibrated Ni-NTA superflow packed column and washed with 10 mM and then 100 mM imidazole to remove nonspecifically bound material. Histidinetagged proteins were eluted with 250 and 500 mM imidazole and dialyzed against 50 mM NaCl, 20 mM HEPES, 10% glycerol, and 1 μg/mL each of aprotinin, leupeptin, and pepstatin for 2 h. The entire purification procedure was performed at 4 °C or on ice.[27]

EGFR kinase assay was set up to assess the level of autophosphorylation based on DELFIA/Time-Resolved Fluorometry. Compounds were dissolved in 100% DMSO and diluted to the appropriate concentrations with 25 mM HEPES at pH 7.4. In each well, 10 *i*L of compound was incubated with 10 μL (5 ng for EGFR) of recombinant enzyme (1:80 dilution in 100 mM HEPES) for 10 min at room temperature. Then, 10 μL of 5× buffer (containing 20 mM HEPES, 2 mM $MnCl_2$, 100 μM Na_3VO_4, and 1 mM DTT) and 20 μL of 0.1 mM ATP-50 mM $MgCl_2$ was added for 1 h. Positive and negative controls were included in each plate by incubation of enzyme with or without ATP-$MgCl_2$. At the end of incubation, liquid was aspirated, and plates were washed three times with wash buffer. A 75 μL (400 ng) sample of europiumlabeled antiphosphotyrosine antibody was added to each well for another 1 h of incubation. After washing, enhancement solution was added and the signal was detected by Victor (Wallac Inc.) with excitation at 340 nm and emission at 615 nm. The percentage of autophosphorylation inhibition by the compounds was calculated using the following equation: 100%−[(negative control)/(positive control−negative control)]. The IC_{50} was obtained from curves of percentage inhibition with eight concentrations of compound. As the

contaminants in the enzyme preparation are fairly low, the majority of the signal detected by the anti-phosphotyrosine antibody is from EGFR.

4.5. Docking study

The three-dimensional structures of the aforementioned compounds were constructed using Chem. 3D ultra 12.0 software [Chemical Structure Drawing Standard; Cambridge Soft corporation, USA (2010)], then they were energetically minimized by using MMFF94 with 5000 iterations and minimum RMS gradient of 0.10. The crystal structures of EGFR kinase (PDB code: (1M17.pdb) complex were retrieved from the RCSBProtein Data Bank (http://www.rcsb.org/pdb/home/home.do). All bound waters and ligands were eliminated from the protein and the polar hydrogen was added to the proteins. Molecular docking of all twenty compounds was then carried out using the Discovery Stutio (version 3.1) as implemented through the graphical user interface CDocker protocol.

Acknowledgements

The work was supported by National Natural Science Foundation of China (Grant No.81102316); the Natural Science Foundation of the Jiangsu Higher Education Institutions of China (Grant No.11KJD350002) and PAPD (A Project Funded by the Priority Academic Program Development of Jiangsu Higher Education Institutions).

References and notes

1. Slamon, D. J.; Clark, G. M.; Wong, S. G.; Levin, W. J.; Ullrich, A.; McGuire, W. L. *Science* **1987**, *235*, 177.
2. Slamon, D. J.; Godolphin, W.; Jones, L. A. *Science (Wash. DC)* **1989**, *244*, 707.
3. Scheurle, D.; Jahanzeb, M.; Aronsohn, R. S.; Watzek, L.; Narayanan, R. H. *Anticancer Res.* **2000**, *20*, 2091.
4. Cox, G.; Vyberg, M.; Melgaard, B.; Askaa, J.; Oster, A.; O'Byrne, K. J. *Int. J. Cancer* **2001**, *92*, 480.
5. Bridges, A. J. *Curr. Med. Chem.* **1999**, *6*, 825.
6. Moscatello, D. K.; Holgado-Mudruga, M.; Godwin, A. K.; Ramirez, G.; Gunn, G.; Zoltick, P. W.; Biegel, J. A.; Hayes, R. L.; Wong, A. J. *Cancer Res.* **1995**, *55*, 5536.
7. Wikstrand, C. J.; McLendon, R. E.; Friedman, A.; Bigner, D. D. *Cancer Res.* **1997**, *57*, 4130.
8. Fry, D. W.; Kraker, A. J.; McMichael, A.; Ambroso, L. A.; Nelson, J. M.; Leopold, W. R.; Connors, R. W.; Bridges, A. J. *Science* **1994**, *265*, 1093.
9. Ward, W. H. J.; Cook, P. N.; Slater, A. M.; Davies, D. H.; Holdgate, G. A.; Green, L. R. *Biochem. Pharmacol.* **1994**, *48*, 659.
10. Bridges, A. J.; Zhou, H.; Cody, D. R.; Rewcastle, G. W.; McMichael, A.; Showalter, H. D. H.; Fry, D. W.; Kraker, A. J.; Denny, W. A. *J. Med. Chem.* **1996**, *39*, 267.
11. Wakeling, A. E.; Barker, A. J.; Davies, D. H.; Brown, D. S.; Green, L. R.; Cartlidge, S. A.; Woodburn, J. R. *Breast Cancer Res. Treat.* **1996**, *38*, 67.
12. Iwata, K.; Miller, P. E.; Barbacci, E. G.; Arnold, L.; Doty, J.; DiOrio, C. I.; Pustilnik, L. R.; Reynolds, M.; Thelemann, A.; Sloan, D.; Moyer, J. D. *Proc. Am. Assoc. Cancer Res.* **1997**, *38*, 633.
13. Woodburn, J. R.; Barker, A. J.; Gibson, K. H.; Ashton, S. E.; Wakeling, A. E.; Curry, B. J.; Scarlett, L.; Henthorn, L. R. *Proc. Am. Assoc. Cancer Res.* **1997**, *38*, 633.
14. *Company Press Release*, Feb 1, **2010**: GSK's TYKERB receives accelerated approval for first-line combination treatment of hormone receptor positive, HER2+/ErbB2+ metastatic breast cancer.
15. Anand, P.; Thomas, S. G.; Kunnumakkara, A. B.; Sundaram, C.; Harikumar, K. B.; Sung, B.; Tharakan, S. T.; Misra, K.; Priyadarsini, I. K.; Rajasekharan, K. N.; Aggarwal, B. B. *Biochem. Pharmacol.* **2008**, *76*, 1590.
16. Huang, M. T.; Lou, Y. R.; Ma, W. *Cancer Res.* **1994**, *54*, 5841.
17. Mukherjee Nee Chakraborty, S.; Ghosh, U.; Bhattacharyya, N. P.; Bhattacharya, R. K.; Dey, S.; Roy, M. *Mol. Cell Biochem.* **2007**, *297*, 31.
18. Pesic, M.; Markovic, J. Z.; Jankovic, D.; Kanazir, S.; Markovic, I. D.; Rakic, L. *J. Chemother.* **2006**, *18*, 66.
19. Hsu, C. H.; Cheng, A. L. *Adv. Exp. Med. Biol.* **2007**, *595*, 471.
20. Garcea, G.; Jones, D. J.; Singh, R.; Dennison, A. R.; Farmer, P. B.; Sharma, R. A. *Br. J. Cancer* **2004**, *90*, 1011.
21. Shishodia, S.; Chaturvedi, M. M.; Aggarwal, B. *Curr. Probl. Cancer* **2007**, *31*, 243.
22. Dorai, T.; Gehani, N.; Katz, A. *Mol. Urol.* **2000**, *4*, 1.
23. Liang, G.; Shao, L. L.; Wang, Y.; Zhao, C. G.; Chu, Y. H.; Xiao, J.; Zhao, Y.; Li, X. Y.; Yang, S. L. *Bioorg. Med. Chem.* **2009**, *17*, 2623.
24. Babasaheb, Y.; Sebastien, T.; Rhonda, J.; Marc, S.; Marc, D.; Tiffany, J. S.; Lesley, L. *Bioorg. Med. Chem.* **2010**, *18*, 6701.
25. Chandru, H.; Sharada, A. C.; Bettadaiah, B. K.; Ananda Kumar, C. S.; Rangappa, K. S.; Sunnila; Jayashree, K. *Bioorg. Med. Chem.* **2007**, *15*, 7696.
26. Jeffrey, D. S.; Christopher, G. V. S.; Caldwell, W. S. *J. Med. Chem.* **1999**, *42*, 3066.
27. Tsou, H.-R.; Mamuya, N.; Johnson, B. D.; Reich, M. F.; Gruber, B. C.; Ye, F.; Nilakantan, R.; Shen, R.; Discafani, C.; DeBlanc, R.; Davis, R.; Koehn, F. E.; Greenberger, L. M.; Wang, Y.-F.; Wissner, A. *J. Med. Chem.* **2001**, *44*, 2719.